Ultrafast millimeter-wave frequency-modulated continuous-wave reflectometry for NSTX

S. Kubota,[a] W. A. Peebles, X. V. Nguyen, and N. A. Crocker
Institute of Plasma and Fusion Research, University of California, Los Angeles, California 90095

A. L. Roquemore
Princeton Plasma Physics Laboratory, Princeton, New Jersey 08543

(Received 8 May 2006; presented on 9 May 2006; accepted 8 August 2006; published online 19 October 2006)

The millimeter-wave frequency-modulated continuous-wave (FM-CW) reflectometer on NSTX is a multichannel system providing electron density profile measurements with a frequency coverage of 13–53 GHz [corresponding *O*-mode density range of $(0.21–3.5)\times10^{13}$ cm^{-3}]. Recently, this system has been modified to allow ultrafast full-band sweeps for repetition intervals down to 10 μs. For this system to function as a fluctuation diagnostic it is crucial to eliminate artifacts in the phase derivative caused by nonlinearities in the frequency sweep; we introduce a simple hardware technique for reducing these artifacts to $\simeq$0.3%. For NSTX, the additional bandwidth ($\leqslant$100 kHz) greatly enhances the capability of the FM-CW reflectometer as a diagnostic for low frequency magnetohydrodynamics instabilities (e.g., internal kinks, resistive wall modes, neoclassical tearing modes, as well as fast-particle driven fishbones and low frequency toroidal Alfvén eigenmodes). © *2006 American Institute of Physics.* [DOI: 10.1063/1.2351894]

I. INTRODUCTION

Reflectometry with the microwave and millimeter-wave range of frequencies is a standard technique for measuring electron density profiles[1,2] and fluctuations[2,3] in fusion plasma devices. In particular, frequency-modulated continuous-wave (FM-CW) reflectometry utilizes the phase derivative from a frequency-modulated source to determine the round-trip propagation time τ of electromagnetic waves between the plasma edge and either the *X*- or *O*-mode cutoff location. For broadband systems, τ versus frequency is then inverted to recover the electron density profile. While the FM-CW systems are the easiest to realize in hardware, the data acquisition and analysis requirements are the most demanding. With the recent availability of fast data acquisition cards ($\geqslant$100 Msamples/s) having gigabytes of onboard memory and continuing trend toward faster processors, this method is being used increasingly as a diagnostic for low frequency oscillations. FM-CW systems with "ultrafast" repetition intervals in the 5–10 μs range have been reported.[4–6]

National Spherical Torus eXperiment (NSTX) is a low aspect ratio ($R/a\sim1.3$) device with auxiliary heating due to neutral beam injection (NBI) up to 6 MW and high harmonic fast wave (HHFW) injection up to 6 MW. Typical device parameters are R_0=85 cm, a=67 cm, I_P=0.7–1.4 MA, and B_T=0.25–0.6 T, with κ=2.0.[7] The unique magnetic geometry of the spherical torus makes NSTX susceptible to an abundance of fast ion driven instabilities ranging in frequency around 10 kHz to several megahertz. While compressional and global Alfvén eigenmodes[8] (CAEs and GAEs) exist in the several hundreds of kilohertz to megahertz range of frequencies, energetic particle modes (EPMs) and toroidal Alfvén eigenmodes[9] (TAEs) are typically found below ~200 kHz. Usually mode structure and amplitude can only be inferred from external magnetic measurements. Some internal measurements exist (Thompson scattering, interferometers, soft x ray, and fixed-frequency reflectometers); however, these diagnostics do not have the combination of spatial coverage, spatial localization, sensitivity, and time resolution of the FM-CW system. The motivation for the upgrades to the FM-CW system is the direct measurement (over a large fraction of the outboard minor radius) of the internal spatial structure and amplitude of these as well as other low frequency magnetohydrodynamics (MHD) instabilities (e.g., internal kinks, neoclassical tearing modes, and resistive wall modes). This information is crucial for better understanding these instabilities as well as for modeling their interactions[10] and effects on fast-particle confinement,[11] which is an important topic for ITER.[12]

The FM-CW reflectometer on NSTX routinely operates with repetition intervals down to 20 μs. In this article we report on modifications enabling us to reach intervals of 10 μs. In addition to the increased bandwidth requirements for sampling the IF signal, fluctuation measurements require high accuracy of the phase derivative measurement (proportional to τ). The linearity of the frequency sweep becomes a key issue since any deviations will create artifacts. In NSTX, TAE fluctuation levels are expected to be $\lesssim$1%. Considering just the *Q*-band (33–53 GHz) system, this translates to maximum fluctuations in τ ranging from 0.5% near the edge to several percent in the core; the measurement error must be much better than this for proper mode structure analysis. In

[a]Electronic mail: skubota@ucla.edu

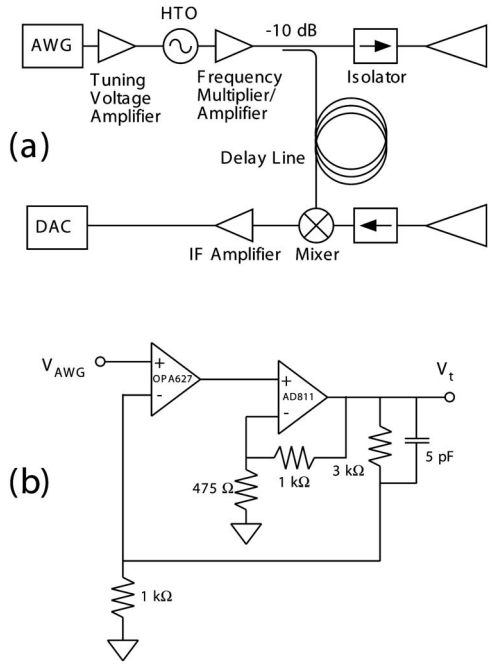

FIG. 1. Schematic of (a) a single channel from the FM-CW reflectometer on NSTX and (b) the HTO driving circuit.

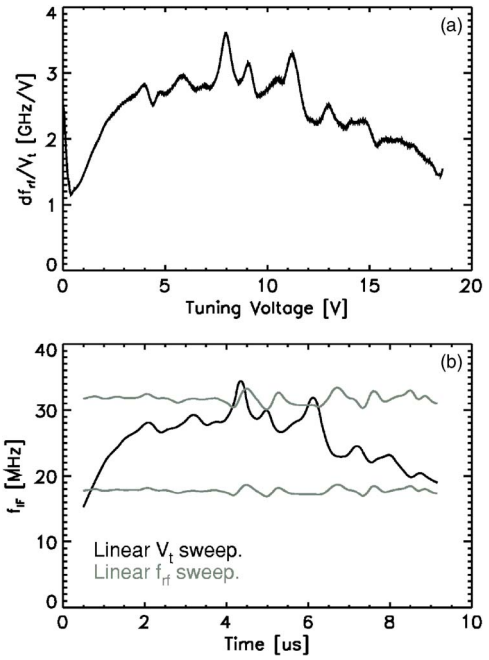

FIG. 2. Plots of (a) the derivative of f_{rf} vs V_t from a static calibration and (b) f_{IF} for a V_t waveform calculated using this calibration to linearize f_{rf}; two curves are shown with a transmission line difference of 24 in. of coaxial cable (corresponding to 2.8 ns in delay time). Also plotted is f_{IF} for a linear V_t sweep. The derivative is shown to accentuate the nonlinearity of the tuning curve. Monuments in df_{rf}/dV_t feed through into f_{IF}.

the following sections we present a description of the diagnostic and provide an iterative technique for correcting much of the above issue in hardware.

II. DIAGNOSTIC DESCRIPTION

Detailed descriptions of the diagnostic hardware[13] and data analysis method[14] are given elsewhere. Figure 1(a) shows a schematic diagram of a single FM-CW homodyne reflectometer channel. Frequency-tunable hyperabrupt varactor-tuned oscillators (HTOs), are used with active frequency multipliers. The tuning voltage (V_t) sweep for the HTO is generated by a computer-controlled Agilent 33220A arbitrary waveform generator (AWG) (14 bit, 64 ksamples, 50 Msamples/s) and amplifier pair. The V_t amplifier uses a composite amplifier design [Fig. 1(b)] to attain a 10 MHz bandwidth at 4× gain. Wide bandwidth amplifiers ($G \gtrsim 45$ dB, 0.05–130 MHz) are used to boost the mixer IF output. The Gage CS12100 data acquisition cards have a maximum sampling speed of 50/100 MHz in single/dual channel mode with 12 bit resolution and 16 Mbytes of onboard memory.

Data are acquired in burst mode with a series of simultaneous pulses triggering both the data acquisition cards and the AWGs for a single upward frequency sweep. For a 10 μs repetition rate, the actual duration of the frequency sweep is ~9 μs, since the AWG has a trigger latency of ~0.5 μs and ~0.5 μs is allotted for the tuning voltage to settle on the downward sweep.

The minimum attainable sweep duration, and hence the maximum attainable repetition rate, is determined by the following: (1) the bandwidth of the IF amplifiers, (2) the sampling rate of the data acquisition, (3) nonlinearity of the tuning curve and modulation frequency of the source, (4) bandwidth of the V_t amplifier, and (5) resolution and bandwidth of the AWG output. Here we will concentrate on items (3)–(5). The AWG is a standard method for linearizing the sweep of the source frequency f_{rf} by applying a predistorted V_t waveform to correct for the nonlinear tuning of the HTO.[16] Ideally the mixer IF signal from a vacuum target is a constant or smoothly varying function of time (or frequency). Figure 2(a) shows a static calibration of frequency f_{rf} versus tuning voltage V_t for the Sivers IMA model 3262X/00 (source for the 33–53 GHz channel). A zeroth order correction linearizes f_{rf} versus time by predistorting the applied V_t waveform using this calibration. The dynamic response of the hardware is different, as is demonstrated by the variations in f_{IF} shown in Fig. 2(b) for a reflection from the center stack.

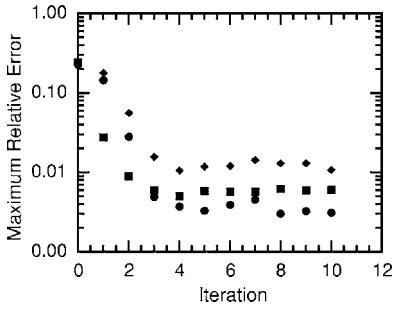

FIG. 3. The decrease in the maximum relative error is shown for three cases: (1) Agilent 33220A and 10 MHz V_t amplifier (●), (2) Agilent 33120A and 10 MHz V_t amplifier (■), and (3) Agilent 33220A and 5 MHz V_t amplifier (♦).

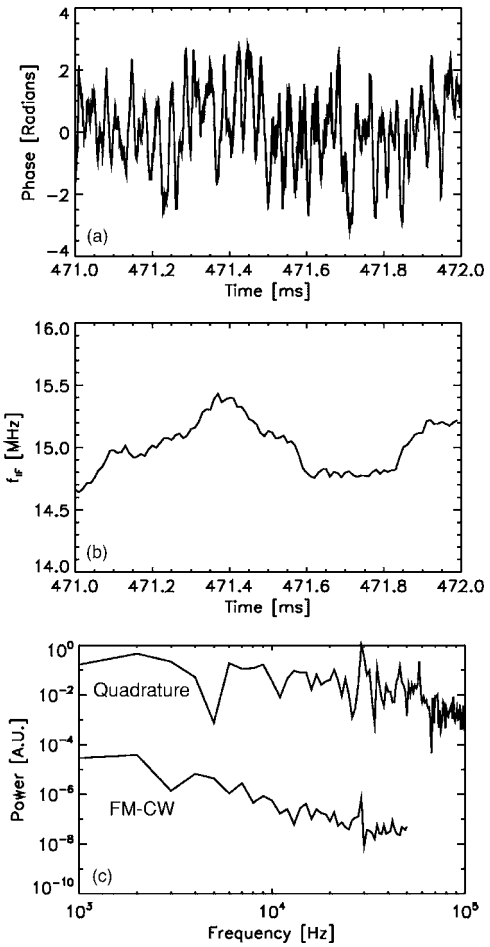

FIG. 4. Plots showing (a) the phase signal from the quadrature 49.8 GHz reflectometer and (b) the time evolution of the f_{IF} from the FM-CW reflectometer for the point closest to this frequency. (c) shows the power spectrum of the two signals.

III. FREQUENCY SWEEP LINEARIZATION

The frequency of the mixer output f_{IF} is determined by the difference between the probe and reference paths. A small nonlinearity $\beta(t)$ added to the frequency sweep at the source

$$f_{rf}(t) = f_0 + \alpha t + \beta(t)t \tag{1}$$

will be propagated to the mixer output

$$f_{IF}(t) = |f_{rf}(t) - f_{rf}(t-\tau)| = \alpha\tau + \beta(t)\tau, \tag{2}$$

where τ is the time delay between the two paths and α is the constant or average f_{rf} sweep rate. Here τ is the desired quantity and the term $\beta(t)\tau$ is the artifact. Figure 2(b) also shows an example of f_{IF} where the delay time has been extended by ~2.8 ns with an additional 24 in. section of coaxial cable in the probe path. Note that the artifact grows proportionally to τ.

Several methods exist in software[17] and hardware[6] for counteracting this effect. The technique used here is an iterative scheme where the V_t ramp is successively corrected to reduce variations in f_{IF} from the center stack reflection. The combination of the optimized V_t waveform along with the HTO can then be used as a linear f_{IF} ramp. Figure 3 shows the relative error of f_{IF} through successive iterations. After about four iterations the method settles to a relative error $\beta(t)/\alpha$ of around 0.3%. Also shown are results for the same technique used with an Agilent 33120A AWG (12 bit, 16000 samples, 40 Msamples/s) as well as when the amplifier cutoff frequency was lowered to 5 MHz. The initial iterations remove the larger and low frequency trends in f_{IF}. The remaining smaller and high frequency corrections rapidly reach the bandwidth and resolution limits of the V_t driving circuitry. Limits due to the modulation bandwidth of the source ($f_m \simeq 13$ MHz) have yet to be assessed. With the expected fluctuation levels for TAEs, it may be necessary to use both methods in conjunction to further decrease the error.

IV. INITIAL MEASUREMENTS

Some technical difficulties prevented us from making measurements with all three channels simultaneously (necessary to perform the profile inversion). Here we will present initial results from the 33–53 GHz channel for an *L*-mode discharge with $n_{e0} \simeq 3.8 \times 10^{13}$ cm^{-3}. Figures 4(a) and 4(b) show the phase signal from a 49.8 GHz channel of the quadrature reflectometers compared with the time evolution of the f_{IF} point for each sweep closest to that frequency. Figure 4(c) shows the power spectrum of the two signals. Note that the oscillations ~30 kHz are clearly visible in both traces. The insensitivity at higher frequencies is possibly due to the finite sampling width of the fast Fourier transform (FFT) window as well as aliasing effects.

The results shown here indicate that additional refinements may reduce measurement errors to levels that allow accurate mode radial profile measurements of fast-particle driven instabilities on NSTX.

ACKNOWLEDGMENT

This work is supported by U.S. DoE Grant No. DE-FG03-99ER54527.

[1] C. Laviron, A. J. H. Donne, M. E. Manso, and J. Sanchez, Plasma Phys. Controlled Fusion **38**, 905 (1996).
[2] E. Mazzucato, Rev. Sci. Instrum. **69**, 2201 (1998).
[3] R. Nazikian, G. J. Kramer, and E. Valeo, Phys. Plasmas **8**, 1840 (2001).
[4] T. Tokuzawa, A. Mase, N. Oyama, A. Itakura, and T. Tamano, Rev. Sci. Instrum. **68**, 443 (1997).
[5] A. Silva *et al.*, Rev. Sci. Instrum. **67**, 4138 (1996).
[6] Ph. Moreau, F. Clairet, J. M. Chareau, M. Paume, and C. Laviron, Rev. Sci. Instrum. **71**, 74 (2000).
[7] M. Ono *et al.*, Nucl. Fusion **40**, 557 (2000).
[8] E. D. Fredrickson *et al.*, Phys. Rev. Lett. **87**, 145001 (2001).
[9] E. D. Fredrickson *et al.*, Phys. Plasmas **10**, 2852 (2003).
[10] N. A. Crocker, W. A. Peebles, S. Kubota, E. D. Fredrickson, S. M. Kaye, B. P. LeBlanc, and J. E. Menard, Phys. Rev. Lett. **97**, 045002 (2006).
[11] E. D. Fredrickson *et al.*, Phys. Plasmas **13**, 056109 (2006).
[12] ITER Physics Basis, Nucl. Fusion **39** (1999).
[13] S. Kubota, X. V. Nguyen, W. A. Peebles, L. Zeng, and E. J. Doyle, Rev. Sci. Instrum. **72**, 348 (2001).
[14] S. Kubota, W. A. Peebles, X. V. Nguyen, N. A. Crocker, and A. L. Roquemore, Rev. Sci. Instrum. **74**, 1477 (2003).
[15] N. A. Crocker, S. Kubota, W. A. Peebles, G. Wang, X. V. Nguyen, and G. J. Kramer, presented at 16th Topical Conference on High Temperature Plasma Diagnostics, Williamsburg, VA, 2006 (unpublished).
[16] K. W. Kim, E. J. Doyle, T. L. Rhodes, W. A. Peebles, C. L. Rettig, and N. C. Luhmann, Jr., Rev. Sci. Instrum. **68**, 466 (1997).
[17] J. Fuchs, K. D. Ward, R. A. York, and M. P. Tulin, IEEE MTT-S Int. Microwave Symp. Dig. **2**, 1175 (1996).